J Neurophysiol 114: 2867–2882, 2015.
First published September 16, 2015; doi:10.1152/jn.00029.2015.

Neuromuscular adjustments of gait associated with unstable conditions

G. Martino,[1,2] Y. P. Ivanenko,[2] A. d'Avella,[2,3] M. Serrao,[4,5] A. Ranavolo,[6] F. Draicchio,[6] G. Cappellini,[1] C. Casali,[5] and F. Lacquaniti[1,2,7]

[1]*Centre of Space Biomedicine, University of Rome Tor Vergata, Rome, Italy;* [2]*Laboratory of Neuromotor Physiology, Istituto di Ricovero e Cura a Carattere Scientifico, Santa Lucia Foundation, Rome, Italy;* [3]*Department of Biomedical Sciences and Morphological and Functional Images, University of Messina, Messina, Italy;* [4]*Rehabilitation Centre Policlinico Italia, Rome, Italy;* [5]*Department of Medical and Surgical Sciences and Biotechnologies, Sapienza University of Rome, Latina, Italy;* [6]*Istituto Nazionale per l'Assicurazione Contro gli Infortuni sul Lavoro, Department of Occupational and Environmental Medicine, Epidemiology and Hygiene, Monte Porzio Catone, Rome, Italy; and* [7]*Department of Systems Medicine, University of Rome Tor Vergata, Rome, Italy*

Submitted 13 January 2015; accepted in final form 11 September 2015

Martino G, Ivanenko YP, d'Avella A, Serrao M, Ranavolo A, Draicchio F, Cappellini G, Casali C, Lacquaniti F. Neuromuscular adjustments of gait associated with unstable conditions. *J Neurophysiol* 114: 2867–2882, 2015. First published September 16, 2015; doi:10.1152/jn.00029.2015.—A compact description of coordinated muscle activity is provided by the factorization of electromyographic (EMG) signals. With the use of this approach, it has consistently been shown that multimuscle activity during human locomotion can be accounted for by four to five modules, each one comprised of a basic pattern timed at a different phase of gait cycle and the weighting coefficients of synergistic muscle activations. These modules are flexible, in so far as the timing of patterns and the amplitude of weightings can change as a function of gait speed and mode. Here we consider the adjustments of the locomotor modules related to unstable walking conditions. We compared three different conditions, i.e., locomotion of healthy subjects on slippery ground (SL) and on narrow beam (NB) and of cerebellar ataxic (CA) patients on normal ground. Motor modules were computed from the EMG signals of 12 muscles of the right lower limb using non-negative matrix factorization. The unstable gait of SL, NB, and CA showed significant changes compared with controls in the stride length, stride width, range of angular motion, and trunk oscillations. In most subjects of all three unstable conditions, >70% of the overall variation of EMG waveforms was accounted for by four modules that were characterized by a widening of muscle activity patterns. This suggests that the nervous system adopts the strategy of prolonging the duration of basic muscle activity patterns to cope with unstable conditions resulting from either slippery ground, reduced support surface, or pathology.

central pattern generator; slippery surface; cerebellar ataxia; muscle synergies; unstable conditions

CONTROL AND COORDINATION OF human walking are the results of the interaction of complex supraspinal and spinal circuitries, under the influence of sensory feedback (Grillner 2011). Experimental evidence has been produced that several kinds of human motor behavior are organized based on the flexible activation of groups of muscles as modules (Davis and Vaughan 1993; Bizzi et al. 2000; Tresch et al. 2002; d'Avella et al. 2003; Drew et al. 2008; Giszter et al. 2010; Lacquaniti et al. 2012; Berger et al. 2013; for an alternative account of empirical findings, see Flanders 2011). Locomotor modules are functional units that generate specific patterns of muscle activation with appropriate timing to efficiently produce motor behaviors (Bizzi et al. 2008). Several studies on locomotion in healthy human adults consistently showed that the electromyographic (EMG) activity of a large number of muscles can be faithfully reconstructed as a linear combination of some basic patterns, each one timed at a different phase of the gait cycle (Davis and Vaughan 1993; Grasso et al. 2004; Cappellini et al. 2006; Monaco et al. 2010; Dominici et al. 2011; Chvatal and Ting 2012; Lacquaniti et al. 2012; Oliveira et al. 2014; Zelik et al. 2014). Muscle activity during locomotion has both invariant and variant features related to the need to compensate for body weight, provide forward and lateral stability, and maintain forward progression (Courtine et al. 2006; McGowan et al. 2010; Ivanenko et al. 2013). The corresponding modules are flexible in both amplitude and temporal envelope, e.g., the duration of muscle activity bursts is scaled and the onset is shifted as a function of walking speed or body weight support (Ivanenko et al. 2004). Moreover, the inclusion of a voluntary task during walking was accomplished by combining activation timings that were associated separately with the voluntary task and locomotion, which was interpreted as a superposition of the locomotor program with the voluntary action program (Ivanenko et al. 2005).

To date, research on motor modules in neuropathological unstable walking has been carried out in poststroke patients (Clark et al. 2010; Gizzi et al. 2011; Kautz et al. 2011; Routson et al. 2014), spinal cord injured patients (Ivanenko et al. 2003; Fox et al. 2013; Hayes et al. 2014; Danner et al. 2015), and patients with Parkinson's disease (Rodriguez et al. 2013). Even though different results emerged from these studies, they revealed an impaired control of muscle activity, most of them reporting a tendency toward reduction of the number of motor modules. Thus Clark et al. (2010) found that poststroke patients show a reduction in modular complexity as a result of a merging of different modules because of the coincident timing, suggesting that cortical lesions lead to inability to independently activate each module. Kautz et al. (2011) and Routson et al. (2014) also showed that in some poststroke subjects the same smaller number of modules contribute to overground and treadmill walking in different conditions. By contrast, Gizzi et al. (2011) in poststroke patients and Ivanenko et al. (2003) in spinal cord injured patients showed a preservation of the activation signals acting on different sets of motor modules. Similarly to Clark et al. (2010), Rodriguez et al. (2013)

Address for reprint requests and other correspondence: G. Martino, Laboratory of Neuromotor Physiology, IRCCS Fondazione Santa Lucia, 306 via Ardeatina, 00179 Rome, Italy (e-mail: g.martino@hsantalucia.it).

studying Parkinson's disease and Danner et al. (2015), Fox et al. (2013), and Hayes et al. (2013) studying spinal cord injured patients identified fewer motor modules compared with healthy subjects, providing evidence for a simplified neuromuscular complexity resulting from dysfunction of different parts of the central nervous system. The previous studies also highlighted plasticity and different solutions to reorganize muscle patterns in both peripheral and central nervous system lesions (Ivanenko et al. 2013).

It is less clear whether the neuromuscular control strategies are also altered in association with unstable balance. Dynamic balance control during locomotion involves complex sensorymotor integration and is influenced by aging, pathology, uneven or slippery terrains, and other factors. To prevent the loss of balance, several compensatory strategies have been found to help maintaining stability: a reduction of walking velocity (Maki 1997; Dingwell et al. 2000), reduction of stride length, increase of stance width (Maki 1997; McAndrew et al. 2012), lowering of the center of mass (McAndrew et al. 2012), and/or prolongation of the double support phase (Maki 1997; Chamberlin et al. 2005). As in the case of walking, postural adjustments during quiet standing have been described by a few motor modules, which are consistent across different biomechanical contexts (Torres-Oviedo and Ting 2010; Safavynia and Ting 2012). In a recent study, it was found that changes in lower limb and trunk kinematics provoked by perturbations during walking were reflected in minimal adjustments in the muscular modular organization, with three of the four modules preserved relative to normal walking (Oliveira et al. 2012). Therefore, the modulation of gait might be influenced by the sensory inputs from perturbations, but the original locomotor program might still be maintained with the addition of new components related to specific biomechanical requirements (Ivanenko et al. 2005; Oliveira et al. 2012).

While many studies succeeded in decomposing motor patterns into a small number of motor modules, a few recent studies have started to shed some light on how and where the weighting coefficients are encoded in the central nervous system (CNS) (Hart and Giszter 2010; Levine et al. 2014) but the way in which the CNS combines modules together is not yet understood. There is still a limited set of data on how the modular architecture of multimuscle activity during walking is modified by different kinds of balance disturbance (but see Chvatal and Ting 2012; Monaco et al. 2012; Oliveira et al. 2012). Here we describe three widely different cases of balance disturbance, two in healthy subjects walking on a slippery walkway (SL) or a narrow beam (NB) and a third one related to cerebellar ataxia (CA). Gait of humans with cerebellar lesions is characterized by irregular unstable patterns, high variability, increased stride width, and high risk of falling (Palliyath et al. 1998; Mitoma et al. 2000; Earhart and Bastian 2001; Stolze et al. 2002; Morton and Bastian 2004; Ilg et al. 2007, 2008; Serrao et al. 2012; Wuehr et al. 2013). On the other hand, slippery surfaces lead healthy individuals to use a cautious gait pattern, with a specific body kinematics and muscular activity (Chambers and Cham 2007; Cappellini et al. 2010). In this case, step length, cycle duration, and horizontal shear forces are significantly smaller, whereas arm movements and trunk oscillations considerably increase compared with normal walking.

In a recent study, we found that CA patients show a widening of muscle activation profiles (Martino et al. 2014). Broader EMG profiles may reflect inaccuracy and variability in the control of individual muscle activation timings or result from modified basic activation patterns. Some basic characteristics of unstable walking have been included in two previous reports (Cappellini et al. 2010; Martino et al. 2014), but the spatiotemporal features of basic activity patterns were not described before. For example, wider EMG bursts in CA may be caused by some temporal overlapping of basic patterns (Clark et al. 2010) that may not necessarily be wider themselves, compared with control patterns. In addition, here we recorded new data and expanded the analysis to different unstable conditions. The aim of the present study was thus to compare the modifications in the spatiotemporal structure of multimuscle EMG activity in patients affected by CA with those in healthy subjects walking on a slippery walkway and on a narrow beam. We hypothesized that the CNS may adopt roughly similar strategies to cope with unstable equilibrium in these three cases; namely, it may prolong the basic muscle activation patterns to increase the overall limb impedance so as to ensure a steadier gait.

MATERIALS AND METHODS

Participants

We describe the results of three separate studies. In the first, we recorded 23 ataxic patients (7 females and 16 males; age range: 32–67 yr; weight: 69 ± 11 kg; means ± SD, leg length 0.78 ± 0.05 m), and 20 age-matched healthy subjects (*control 1* group: 7 females and 13 males; age range: 34–70 yr; weight: 70 ± 14 kg; leg length: 0.80 ± 0.05 m). Thirteen patients had a diagnosis of autosomal dominant ataxia (spinocerebellar ataxia, 7 pts with SCA1, 6 pts with SCA2), while the other 10 patients had sporadic adult onset ataxia of unknown etiology (SAOA). Even if extracerebellar involvement is common in both SCA1 and 2, none of our patients had clinically significant signs other than the cerebellar ones. In particular, they did not show extrapyramidal or pyramidal signs nor signs of peripheral nerve or muscle deficits, which tend to be overt over the course of the disease. Disease severity was measured by means of Inherited Cerebellar Ataxia Rating Scale (ICARS) (Trouillas et al. 1997). Magnetic resonance imaging of all patients showed pan-cerebellar degenerations with significant atrophy of the cerebellar vermis. All patients were undergoing standard physical therapy, which included upper and lower limb exercises, balance, and gait training. Nineteen patients with mild to moderate severity (ICARS $\leq$30) represented the main group for comparison with healthy subjects at matched walking conditions. Four more severe patients (ICARS $>$30) required walking assistance (hand contact with the experimenter) and walked significantly slower; therefore, they were analyzed separately.

In the second study, we recorded eight healthy volunteers walking on a slippery surface (2 females and 6 males; age range: 30–48 yr; weight: 74 ± 10 kg; leg length: 0.80 ± 0.03 m). The general kinematic and EMG data of five of these subjects have been documented previously (Cappellini et al. 2010). Here, we recorded three new subjects in the same experimental conditions as in the previous study to increase the sample size.

In the third study, we recorded 10 healthy volunteers walking on a narrow beam (6 females and 4 males; age range: 26–43 yr; weight: 65 ± 11 kg; leg length: 0.86 ± 0.08 m).

None of the healthy subjects had any history of neurologic or orthopedic disease. All participants provided written informed consent to procedures approved by the local Ethics Committee, in conformity with the Declaration of Helsinki on the use of human subjects in research.

Procedures and Data Recording

Study 1. All subjects were asked to walk barefoot along a walkway, ~7-m length, while looking forward. They walked at comfortable self-selected speeds but were encouraged to walk also at the fastest speed at which they still felt safe, resulting in a range of different speeds across the recorded trials. Given that typical walking speeds were rather slow in CA patients, we instructed the healthy controls (*control 1* group) to walk at different speeds, including slow ones so as to roughly match the walking speed of CA patients. To ensure safe walking conditions, an assistant walked alongside the subjects when necessary. Groups of 3 trials were separated by 1-min rest periods to avoid muscle fatigue and at least 15 trials were recorded for each subject. Kinematic data were recorded bilaterally at 300 Hz using an optoelectronic motion analysis system (SMART-D System; BTS, Milan, Italy) consisting of eight infrared cameras spaced around the walkway. Ground reaction forces were recorded at 1,200 Hz by means of two force platforms (0.6 m × 0.4 m; Kistler 9286B, Winterthur, Switzerland), placed at the center of the walkway, attached to each other in the longitudinal direction, but displaced by 0.2 m in the lateral direction. The EMG data were recorded at 1,000 Hz using a wireless system (FreeEMG300 System; BTS).

Study 2. For the slippery condition, we uniformly applied oil across the entire surface of a polyethylene film coating the laboratory floor, so that it formed a thin layer on the walkway without spilling off the walking path (Cappellini et al. 2010). Participants wore shoe covers over their bare feet that were made from the same thin polypropylene material used for the floor to reduce the interface friction. In the middle of the walkway, subjects stepped on a force plate. The measured ground reaction shear forces were not significantly affected by the presence of the polyfilm covering the force plate. The operational dynamic coefficient of friction during walking on the slippery surface, estimated as the mean ratio of the shear to normal foot force (Heiden et al. 2006) during late stance of the gait cycle (measured when the foot slightly slipped in the lateral direction), was 0.06 ± 0.1 (Cappellini et al. 2010). For comparison, for slippery conditions on level surfaces, this ratio was reported to be as low as 0.02 (a fall case), compared with ~0.2 for grip trials (Strandberg 1983; Grönqvist et al. 1993; Redfern et al. 2001). No practice was allowed before the recordings. Thirteen consecutive trials of walking on the slippery surface at a natural speed were recorded in each subject. Before walking on the slippery surface, the subjects were asked to walk on the normal floor (*control 2*) at relatively slow speeds (10 trials) to roughly match walking speeds (Fig. 1*B*). Kinematic data were recorded bilaterally at 100 Hz by means of the Vicon-612 system (Oxford, UK). Nine TV cameras were spaced around the walkway. The ground reaction forces were recorded at 1,000 Hz by a force platform (0.9 × 0.6 m; Kistler 9287B, Zurich, Switzerland). The EMG activity was recorded using active Delsys electrodes (Delsys, Boston, MA).

Study 3. For the beam walking condition, participants walked barefoot along a narrow metal beam (6-m length, 4-cm width, and 4-cm height) at comfortable self-selected speeds. No practice was allowed before the recordings. Ten consecutive trials of walking on the beam were recorded in each subject. Before walking on the beam, the subjects were also asked to walk on the normal floor (*control 3*) at relatively slow speeds (10 trials; Fig. 1*B*). Kinematic data were recorded bilaterally at 100 Hz by means of the Vicon-612 system. Nine TV cameras were spaced around the walkway. The EMG activity was recorded using wireless Delsys electrodes (Trigno).

In all studies, infrared reflective spherical markers (15 mm in diameter) were attached on each side of the subjects to the skin overlying the following landmarks: gleno-humeral joint (GH), greater trochanter (GT), lateral femur epicondyle (LE), lateral malleolus (LM), heel (HE), and fifth metatarso-phalangeal joint (VM). EMG activity was recorded by means of surface electrodes applied to lightly abraded skin over the respective muscle belly from 12 muscles simultaneously on the right side of the body in each subject. The following 12 muscles were recorded: tibialis anterior (TA), gastrocnemius lateralis (LG), gastrocnemius medialis (MG), soleus (SOL), peroneus longus (PL), vastus lateralis (VL), vastus medialis (VM), rectus femoris (RF), biceps femoris (long head, BF), semitendinosus (ST), tensor fascia latae (TFL), and gluteus medius (GM). Electrode placement was carefully chosen to minimize cross talk from adjacent muscles during isometric contractions (Ivanenko et al. 2006). Sampling of kinematic, force platform, and EMG data was synchronized.

Data Analysis

Cycle definition. Gait cycle was defined as the time between two successive foot-floor contacts by the same leg. For gait on normal ground and on narrow beam, foot strike and lift-off events were determined from maximum and minimum excursions of the lower limb elevation angle (Borghese et al. 1996; Vasudevan et al. 2011), defined as the angle between the vertical axis and the whole limb segment (from the greater trochanter to lateral malleolus), projected on the sagittal plane. For the slippery condition, instead, foot strike was determined according to the local minima of the vertical displacement of the HE marker (Ivanenko et al. 2007), while the timing of the lift-off was determined when the VM marker was raised by 3 cm. When subjects stepped on the force platforms, these kinematic criteria were verified by comparison with foot strike and lift-off estimated from the vertical ground force, namely when this force exceeded a threshold of 7% of body weight. In general, the difference between the time events measured from kinematics and kinetics was $< 3\%$ in all conditions.

Kinematic data processing. For the analysis of locomotor patterns, the steps related to gait initiation and termination were discarded and only those performed in the central section of the path at roughly constant speed were included in the analysis. The following general gait parameters were calculated for each subject: walking speed, cycle duration, stride length, and stride width. We also computed the anatomical joint angles of the limb segments and the roll angle of the trunk. From these variables, we derived the range of angular motion (RoM). The kinematic data were time interpolated over individual gait cycles to fit a normalized 200-point time base.

EMG activity and basic activation patterns. Basic activation patterns were extracted from the EMG envelopes using the non-negative matrix factorization (NNMF) algorithm (Lee and Seung 2001). The raw EMG signals were band-pass filtered using a zero-lag third-order Butterworth filter (20–450 Hz), demeaned, rectified and low-pass filtered with a zero-lag fourth-order Butterworth filter (10 Hz). The time scale was normalized by interpolating individual gait cycles over 200 points. For each subject, the EMG signal from each muscle was normalized to its peak value across all trials. The processed EMG envelopes were combined into an $m \times t$ matrix M (where m is the number of muscles and t is 200 × number of gait cycles collected across all trials). Thus the NNMF was applied to all strides of each subject to identify the underlying basic activation patterns (P) in the EMG recordings. The algorithm looks for an approximate solution

$$M \cong W \times P \quad (1)$$

where M is assumed to be a linear composition of basic activation patterns P ($n \times t$ matrix, where n is the number of basic patterns) and weighting coefficients or muscle synergies W ($m \times n$ matrix). The W and P are estimated to minimize the root-mean-squared residual between M and $W \times P$. The factorization uses an iterative method starting with random initial values for W and P. Because the root-mean-squared residual may have local minima, the best solution was selected out of 100 runs to find W and P from multiple random starting values. Each run of the NNMF was executed until a termination tolerance on change in size of the residual or in the elements of W and P set to 10^{-5}.

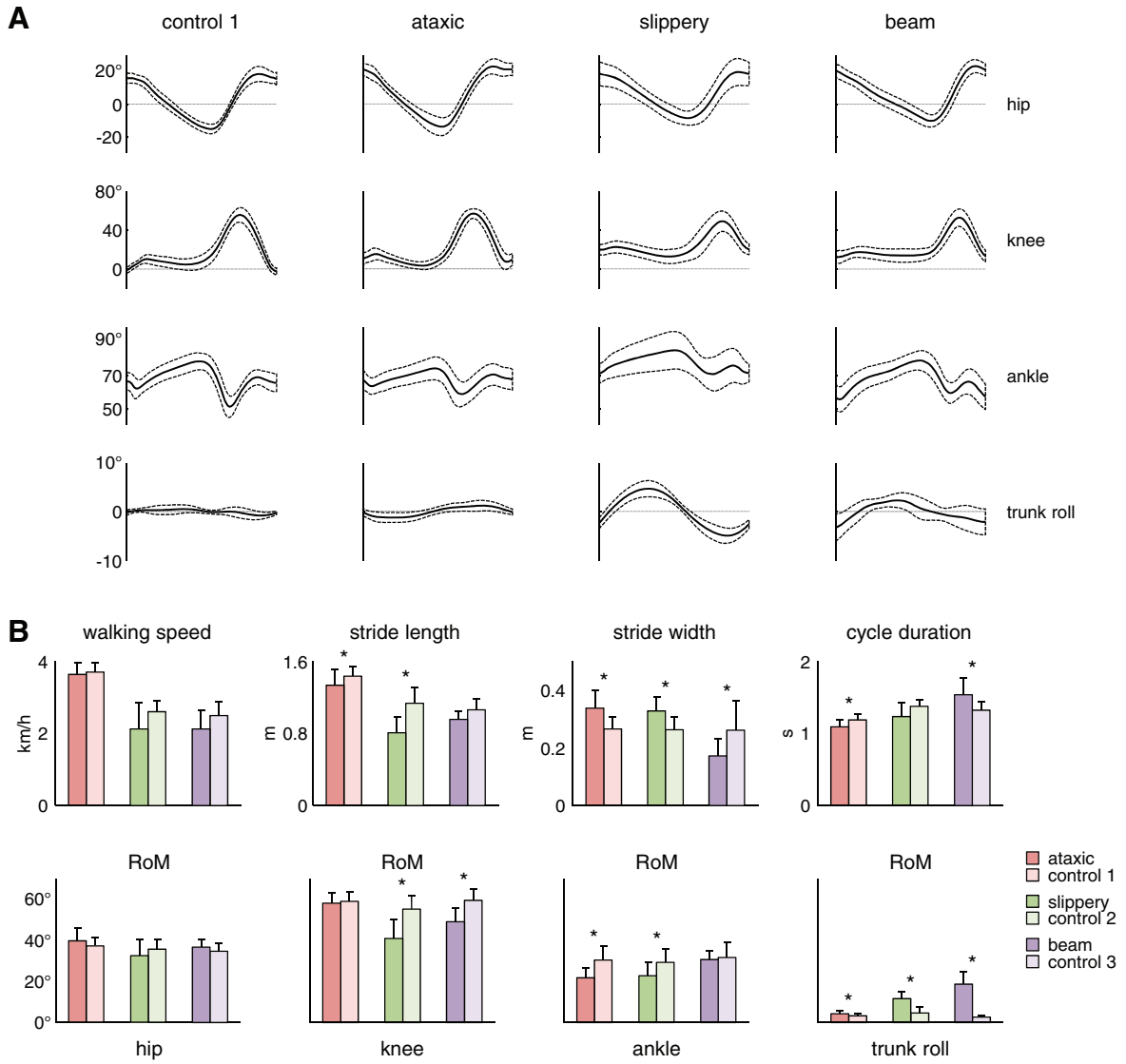

Fig. 1. Kinematics gait parameters. *A*: ensemble-averaged (means ± SD) hip, knee, and ankle joint and trunk roll orientation angles in 20 healthy subjects (*control 1* group), 19 cerebellar ataxic patients [International Cooperative Ataxia Rating Scale (ICARS) ≤30], and healthy subjects walking along a slippery walkway and on beam. *B*: comparison of general gait parameters for ataxic patients and healthy subjects during unstable walking (slippery, beam), relative to respective control groups at matched walking speeds. Data were normalized to the cycle duration and represented in percent of gait cycle (from touchdown to successive touchdown). RoM, range of motion. $*P < 0.05$, significant differences.

The basic activation patterns were then segmented back into individual cycles ($n \times 200$) for averaging or for individual stride analysis. The patterns were grouped and plotted in a chronological order (i.e., according to the timing of the main peak relative to the normalized gait cycle). To identify and average similar basic patterns across subjects, the degree of similarity was evaluated based on the best-matching scalar product of weighting coefficients normalized to the Euclidean norm (Cheung et al. 2005). Briefly, we first computed the best-matching scalar products between each individual synergy set and the mean of randomly ranked interindividual sets. Then, we iteratively updated this mean by comparing every possible combination and finding the one that maximized the total scalar product. If synergies from one set were not matched to the synergies from the mean set (scalar product <0.6), we isolated those unmatched synergies (see *Comparison of Basic Activation Patterns and Muscle Synergies in CA, SL, and NB* in the RESULTS).

Pattern decomposition was assessed by calculating the percent of variability [or variance (VAF)] accounted for (Torres-Oviedo et al. 2006):

$$\text{VAF} = \text{sum of squared errors}/\text{total sum of squares} \quad (2)$$

where the total sum of squares is taken with respect to the mean over the rows of the data matrix. To determine the minimum number of basic activity patterns n, which best accounts for the EMG data variance, we used a method ("best linear fit") based on a linear regression procedure (d'Avella et al. 2006) by varying the number of basic patterns from 1 to 8 and selecting the smallest n such that a linear fit of the VAF vs. n curve had a residual mean square error $<10^{-4}$. To characterize differences in the duration of EMG activity and basic patterns between groups, we computed the full width at half maximum (FWHM). The FWHM was calculated as the sum of the durations of the intervals in which the rectified EMG or the basic activation patterns (after subtracting the minimum throughout the gait cycle) exceeded half of its maximum.

To characterize the phase of basic activation patterns with respect to the gait cycle, we calculated its center of activity (CoA) (Martino et al. 2014; Sylos-Labini et al. 2014). The CoA was chosen because it was impractical to reliably identify a single peak of activity in some

pathological subjects and during unstable conditions. The CoA during the gait cycle was calculated using circular statistics (Batschelet 1981) and plotted in polar coordinates (polar direction denoted the phase of the gait cycle, with angle θ that varies from 0 to 360°). It was calculated as the angle of the vector (1st trigonometric moment) that points to the center of mass of that circular distribution using the following formulas:

$$A = \sum_{t=1}^{200} \left(\cos\theta_t \times P_t\right) \quad (3)$$

$$B = \sum_{t=1}^{200} \left(\sin\theta_t \times P_t\right) \quad (4)$$

$$\mathrm{CoA} = \tan^{-1}\left(B/A\right) \quad (5)$$

The CoA can only be considered as a qualitative parameter, because averaging between distinct foci of activity may lead to artificial activity in the intermediate zone. Nevertheless, it can be helpful to understand if the distribution of activity remains unaltered across different groups and conditions.

Statistics

Between groups differences in the spatiotemporal gait parameters and FWHM were assessed by performing unpaired two-sample *t*-tests in *study 1* and paired *t*-tests in *study 2* and in *study 3*. The analysis of CoA was performed using the Watson-Williams test for circular data (Watson and Williams 1956). The correlation among kinematics, muscle activation patterns, and clinical scores was performed using Spearman's rank correlation coefficient. Between group similarities in both temporal basic activation patterns and muscle synergies was assessed by measuring the scalar product between them (after normalization to unit vectors). Descriptive statistics included means ± SD, and significance level was set at $P < 0.05$. All statistical analyses were performed using Statistica (v7.0) and custom software written in Matlab (v8.1).

RESULTS

General Gait Parameters in Ataxic Gait (Study 1)

Figure 1*A*, *left*, shows the ensemble-averaged kinematic patterns of hip, knee, and ankle joint and trunk roll orientation angles in CA patients ($n = 19$, ICARS ≤30) and the age-matched control subjects (*control 1*). The time course of changes of hip and knee joint angles of CA was very similar to that of healthy subjects. In contrast, a substantial reduction of the ankle joint excursion ($P < 0.0001$) and increment of oscillations in the trunk roll angle ($P < 0.001$) were observed in CA relative to controls (Fig. 1*B*). At matched walking speeds, cerebellar patients showed a significant increase in the stride width and reduction in the cycle duration and stride length compared with healthy controls (Fig. 1*B*). These results are consistent with previous studies (Palliyath et al. 1998; Mitoma et al. 2000; Serrao et al. 2012).

EMG Envelopes and Basic Activation Patterns

We recorded EMG signals from 12 muscles of the right lower limb. Figure 2*B* illustrates raw EMG traces in one CA patient during two consecutive strides. The normalized and ensemble-averaged EMGs for CA and controls are illustrated in Fig. 3*A*. The activity of hamstring muscles (BF and ST) in patients tended to be higher during the swing phase and was prolonged till about 50% of gait cycle with respect to the healthy subjects (Fig. 3*A*). A wider activity was also notable in the TA muscle. Similarly, extensor ankle muscles (SOL, MG, LG, and PL) in CA showed activity throughout the whole stance phase, even at the onset of stance, i.e., at a time when they were silent in controls. The analysis of FWHM allowed us to quantify the duration of activity of each muscle. Figure 4*B* shows that most muscles (TA, hamstrings, and ankle extensors) significantly increased their FWHM in CA patients compared with healthy subjects.

The analysis of dimensionality using the NNMF method showed that EMG activity changes during walking are adequately captured by a small number of motor modules in both healthy subjects and CA patients (Fig. 5*A*). Even if three or five modules were sufficiently representative in a few subjects, we reported only the analysis considering four basic patterns in all participants, since EMG activity in most subjects was well accounted for by four modules (Fig. 5*B*). The percent total variance accounted for by four basic patterns was 85 ± 2.4% in controls ($n = 20$) and 85.4 ± 2.7% in CA ($n = 19$; ICARS ≤30). We separately analyzed the group of severe patients ($n = 4$; ICARS >30) since they walked significantly slower (on average 1.6 km/h) and/or with the arm support of the experimenter. Also, the EMG activities of these patients involved four modules (Fig. 5*B*).

The basic activation patterns and corresponding weightings (muscle synergies) are reported in Fig. 5, *C* and *D*. The muscle weightings and pattern activation timing were generally similar between groups. Each basic pattern peaked at a particular time of the gait cycle and showed specific characteristics. Pattern P1 mainly loaded on RF, VL, VM, GM, and TFL muscles and peaked around heel strike, providing body support during weight acceptance. Pattern P2 mainly loaded on the ankle extensor muscles (SOL, MG, LG, and PL) and contributed to limb loading and propulsion. Pattern P3 was primarily related to the activity of TA and TFL during swing. Pattern P4 was mainly involved in the modulation of hamstrings (BF and ST) during late swing and early stance. The FWHM was significantly greater ($P < 0.006$) for P2, P3, and P4 in CA (Fig. 5*E*), reflecting a similar widening of the EMG envelopes (Figs. 3*B* and 4*B*). In severe patients, the FWHM of P1, P2, and P4 was also significantly greater than in controls (Fig. 5*E*).

We reported the analysis considering four basic patterns in all participants (Fig. 5), but it is noteworthy that this choice did not affect the main result of a prolongation of basic muscle activation patterns in CA. Indeed, when we used three or five modules, the FWHM of these modules was still remarkably larger than in controls, exceeding their 95% confidence interval. Finally, as we indicated in MATERIALS AND METHODS, the EMG signal from each muscle was normalized to its peak value across all trials. In line of principle, this normalization procedure might affect the determination of the number of modules and/or their burst duration. Therefore, we verified whether widening of basic patterns in CA could depend significantly on EMG normalization or on a threshold for characterizing their duration. To this end, we performed the NNMF analysis on non-normalized EMG data (in μV). The number of significant modules in most subjects (~63%) remained four and their duration, estimated either by the FWHM or by the average duty cycle [when activity exceeded 0.15 of maximum, Hayes et al. (2014)] was still significantly greater in CA for P2,

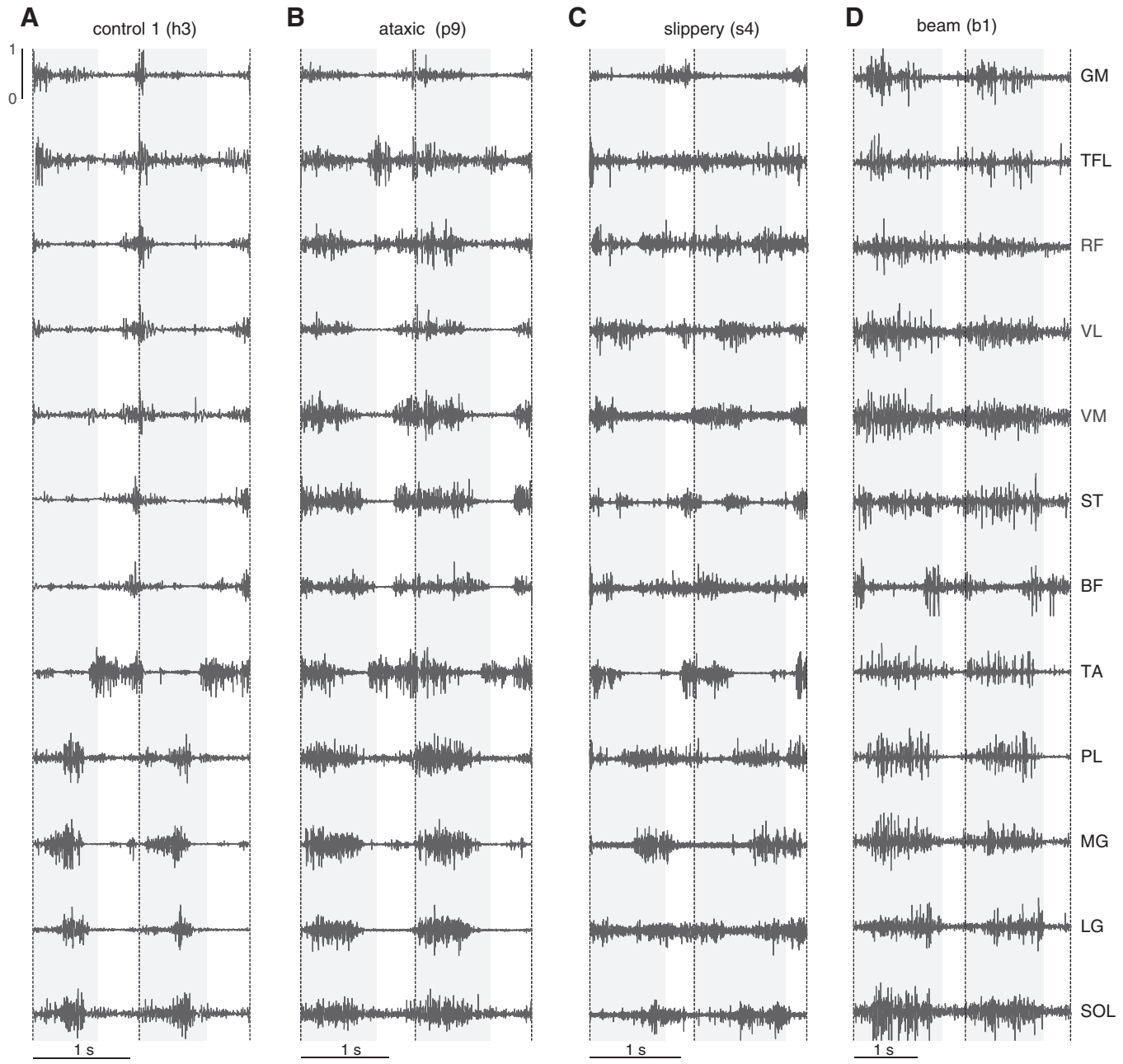

Fig. 2. Example of EMG traces in one representative control *subject h3* (*A*), 1 CA *patient p9* (*B*), 1 subject on a slippery *surface s4* (*C*), and 1 subject walking on a *beam b1* (*D*) during 2 consecutive strides. The stance phase is evidenced by a shaded region in each case and EMGs were normalized to their max value across all trials.

P3, and P4; $P < 0.008$ when using the FWHM and $P < 0.003$ when using the 0.15 max threshold.

Correlations Between Basic Activation Patterns, Gait Parameters, and Clinical Scores in CA

We observed significant relationships ($P < 0.02$) between mean FWHM (across all basic patterns) and cycle duration, stride length, and stride width of CA patients (Fig. 6*A*). We found also significant correlation between clinical ICARS measures and mean FWHM of basic activation patterns ($P = 0.001$; Fig. 6*B*). Including more severe patients ($n = 4$, ICARS >30) increased the correlation between clinical ICARS measures and mean FWHM ($P = 0.0004$), likely because P1 and P4 basic patterns were wider in these patients than in the less severe patients (Fig. 5*E*). In sum, wider basic activation patterns in CA gait correlated with the severity of pathology.

General Gait Parameters of Walking on the Slippery Surface (Study 2)

Here, we used a similar analysis to characterize walking of healthy subjects on a slippery surface (SL). The temporal changes in the ensemble-averaged kinematic patterns of knee and ankle angles demonstrated a significant reduction of all the respective RoM ($P < 0.02$) and a high variability across subjects (Fig. 1, *A* and *B*), although the trajectories of

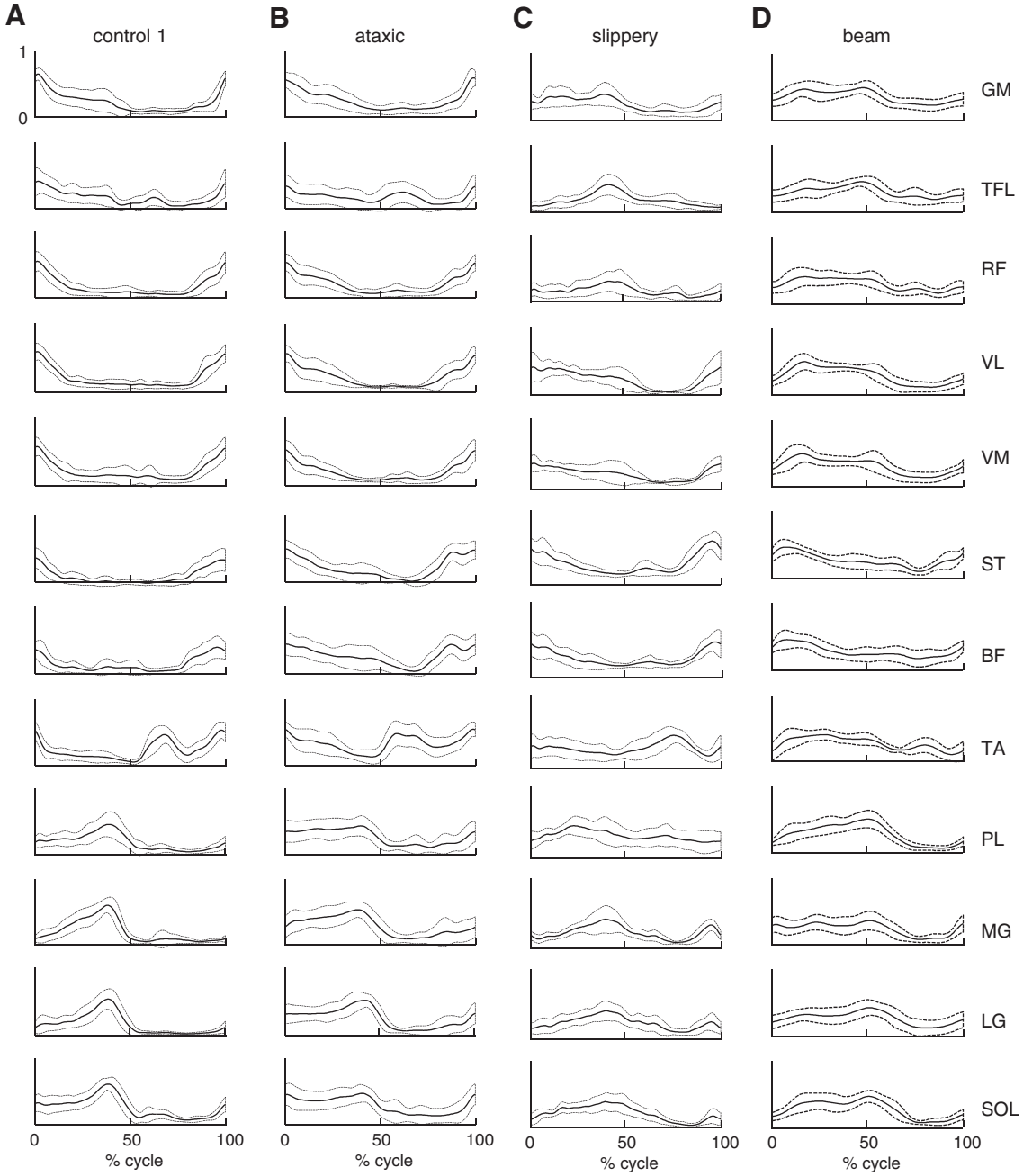

Fig. 3. Ensemble averaged (±SD) EMG activity patterns of 12 ipsilateral leg muscles recorded from *control*' group (*A*), ataxic patients (*B*), and healthy subjects during slippery (*C*) and beam (*D*) walking. EMGs were normalized to their max value across all trials. EMG data are plotted vs. normalized gait cycle. GM, gluteus medius; TFL, tensor fascia latae; RF, rectus femoris; VL, vastus lateralis; VM, vastus medialis; ST, semitendinosus; BF, biceps femoris; TA, tibialis anterior; PL, peroneus longus; MG, gastrocnemius medialis; LG, gastrocnemius lateralis; SOL, soleus.

the limb segment angles were still similar to those of normal walking. Even at matched speeds, the stride length was significantly shorter on the slippery surface than that on the normal one (Fig. 1*B*). Foot motion on the slippery surface resembled that of a nonplantigrade gait (without heel-to-toe rolling pattern) (Cappellini et al. 2010) and was characterized by a significantly larger stride width (Fig. 1*B*) due to slips in the stance phase. Consistent and systematic trunk tilts in the frontal plane were typical features of walking on the slippery surface (Fig. 1, *A* and *B*). This is in contrast with normal walking, where both the hip and shoulder move in concert, resulting in parallel lateral trunk shifts without noticeable inclinations. On the slippery surface, lateral oscillations increased in all subjects, resulting in the prominent trunk roll in the frontal plane (Fig. 1*B*; $P < 0.07$).

EMG Envelopes and Basic Activation Patterns

An example of muscle activation patterns in SL is illustrated in Fig. 2*C*, while the ensemble-averaged EMGs are shown in Fig. 3C. The pattern and sequence of activation of individual muscles were different on the slippery surface. Notice, for instance, the differences in midstance activity in the TFL, GM, BF, VL, VM, and RF for the slippery surface (Fig. 3*C*).

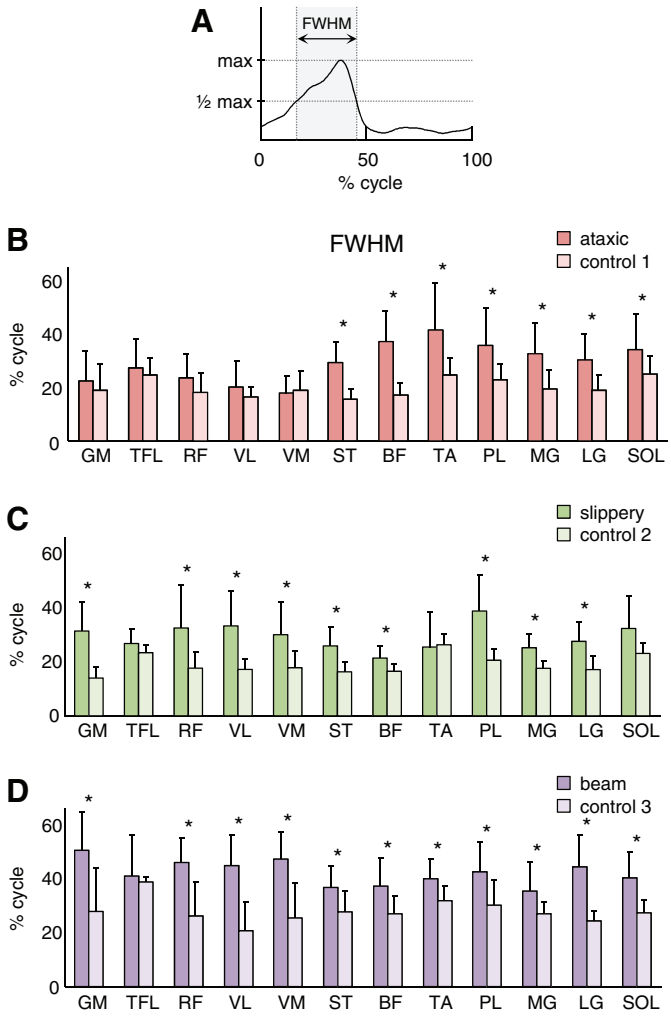

Fig. 4. Full width at half maximum (FWHM) of leg muscle EMGs (means ± SD) for ataxic patients (*B*) and healthy subjects during slippery (C) and beam (*D*) walking conditions compared with respective control groups. FWHM was calculated as the duration of the interval (in percent of gait cycle) in which EMG activity exceeded half of its maximum (*A*). *Significant differences.

Similarly to CA gait, calf muscle activations in SL were prolonged. In particular, the analysis of FWHM showed a significant broader activity in most muscles in subjects walking on the slippery surface vs. that walking on normal floor (Fig. 4*C*).

In both control and SL conditions, EMG activity changes were adequately captured by a small number of motor modules (Fig. 7, *A* and *B*). The "best linear fit" criteria showed that EMG activity for walking on both normal and slippery surface required four modules on average. The VAF by four basic patterns was 83.8 ± 4.9% in SL and 85.2 ± 2.1% during normal walking.

Figure 7, *C* and *D*, shows the muscle weightings and pattern activation timing. While the muscle weightings were generally similar between walking conditions, we found some differences in the profiles of activity patterns. Patterns P1 and P4 showed prolonged activation for the SL condition in late and early stance, respectively (Fig. 7*C*). P2 also showed some activity in early and late swing in SL. Pattern P3 showed a higher activity during almost all the gait cycle except for the touchdown timing. The FWHM was significantly greater ($P < 0.01$) for P1, P2, and P4 in SL (Fig. 7*E*), reflecting similar properties of the EMG envelopes (Fig. 4*C*).

Some differences in the kinematics can occur between the first and last trials due to adaptation to the SL condition [e.g., in the amplitude of lateral hip and trunk oscillations (Cappellini et al. 2010)]. Therefore, we verified whether there could also be some changes in the FWHM parameter across trials. Even though walking experience might decrease gait instability and kinematic variability (Cappellini et al. 2010), we did not find significant differences in the FWHM of P1–P4 between the first and last trial of SL in our subjects ($P > 0.14$), and the FWHM remained significantly greater ($P < 0.0001$) in the last trial of SL than in normal walking.

General Gait Parameters of Walking on Narrow Beam (Study 3)

At matched walking speeds, beam walking was characterized by decreased stride width, longer cycle duration, reduced range of motion in the knee joint, and increased trunk oscillations compared with normal overground walking (Fig. 1*B*). As for slippery surface walking, the leg (knee joint) was somewhat flexed during stance (by ~10–15°; Fig. 1*A*) and the temporal changes in the kinematic patterns were more variable than during normal walking, reflecting the postural instability induced by the narrow beam. However, in contrast to decrements in the stride length for CA and SL, the stride length was similar between beam and overground walking at matched walking speeds (Fig. 1*B*).

EMG Envelopes and Basic Activation Patterns

An example of muscle activation patterns in beam walking is illustrated in Fig. 2*D* and the ensemble-averaged EMGs are shown in Fig. 3*D*. As in the case of SL walking, there was a substantial midstance activity of many muscles (e.g., GM, TFL, RF, VL, VM, ST, BF, and TA) in NB (Fig. 3*D*). Similarly to CA and SL gait, calf muscle activations in NB were prolonged. The analysis of FWHM showed a significant broader activity in almost all muscles in subjects walking on the beam vs walking on normal floor (Fig. 4*D*).

In both control and NB conditions, EMG activity changes were adequately captured by a small number of motor modules (Fig. 8, *A* and *B*). The best linear fit criteria showed that EMG activity for both normal and beam walking required four modules in most subjects (>70%). The VAF by four basic patterns was 85.0 ± 2.8% in NB and 83.8 ± 3.8% during normal walking.

Figure 8, C and *D*, shows the muscle weightings and basic activation patterns. While the muscle weightings (W) were generally similar between walking conditions (although W1 and W3 were more variable; Fig. 8*D*), the profiles of activity patterns differed. In particular, pattern P1 and P3 showed considerable activity in midstance. The FWHM was significantly greater ($P < 0.01$) for all basic patterns in NB (Fig. 8*E*). The FWHM of P1–P3 patterns did not differ between the first and last trials of NB ($P > 0.44$) while that of P4 slightly decreased ($P < 0.01$). Nevertheless, the FWHM of P4 remained greater than that during normal walking ($P < 0.01$).

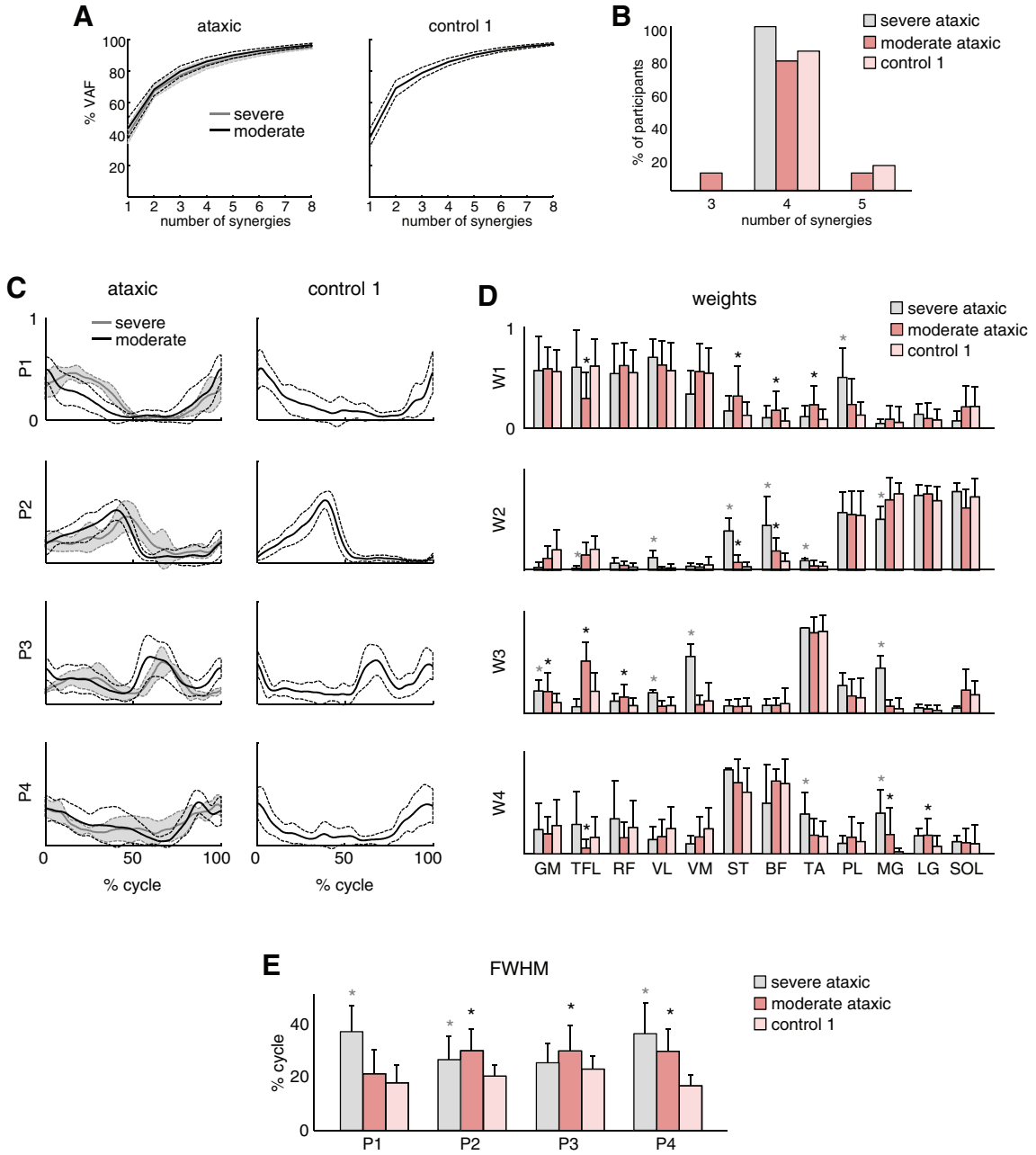

Fig. 5. Statistical analysis of EMG patterns in cerebellar ataxic (CA) using non-negative matrix factorization (NNMF). *A*: cumulative percent of variance (VAF; ±SD) explained by basic EMG components in ataxic patients (*left*) and healthy controls (*right*). The data for the main group of ataxic patients ($n = 19$, ICARS ≤30) and severe ataxic patients (ICARS >30, $n = 4$) are shown separately. The VAF value is calculated as 1 − SSE/SST, where SEE (sum of squared errors) is the unexplained variation and SST (total sum of squares) is the total variation of the data. *B*: number of modules needed to account for cycle-by-cycle variability of muscle activity estimated using the best linear fit method. The majority of healthy subjects and ataxic patients needed 4 modules. *C*: ensemble-averaged basic temporal patterns (±SD) of ataxic patients and controls with four modules assumed for each group. Basic patterns were plotted in a "chronological" order (with respect to the timing of the main peak). *D*: corresponding muscle weights. *E*: FWHM (means ± SD) of the basic temporal patterns. *Significant group differences.

Comparison of Basic Activation Patterns and Muscle Synergies in CA, SL, and NB

In addition to comparison with the respective control groups (Figs. 5, 7, and 8), we also quantified similarities in muscle synergies [weights (W)] and basic temporal patterns (P) between CA patients and healthy subjects walking on a slippery surface and beam. To this end, we used scalar products (Cheung et al. 2009) between individual synergies with mean synergies of each group (Fig. 9*A*). The number of modules for each subject was not constrained to four a priori, but was selected a posteriori based on the best linear fit method. Muscle synergies were grouped based on their best similarities. Synergies 1, 2, 4, and 6 were identified in each group, while synergies 3, 5, and 7 were identified only in some groups (Fig. 9*A*). The synergies extracted from each individual were generally similar to the mean synergy vectors of his or her own group (see the mean scalar product of weights of individual subjects with the group mean weight in Fig. 9*A*, *top*, on average, 0.93 ± 0.04 for CA [range 0.82–0.99], 0.92 ± 0.04

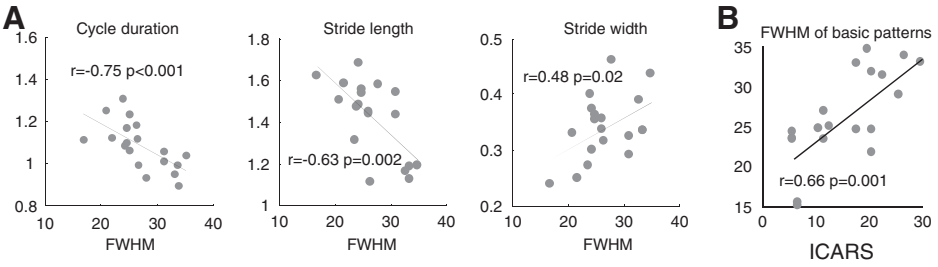

Fig. 6. Clinical correlations. Significant kinematics electromyographic parameters in ataxic patients ($n = 19$) as a function of the ICARS total score. Each point represents the mean value for an individual patient. Linear regression lines with corresponding r and p values are reported. *B*: averaged FWHM of all patterns vs. the ICARS total score.

for SL [range 0.72–0.98], and 0.89 ± 0.07 for NB [range 0.71–0.98]). This analysis also confirmed that there were four consistent synergies (high percentage of subjects showing them) in all conditions, the remaining synergies were inconsistent across subjects (depicted with low-tone colors in Fig. 9). However, the consistent synergies in each group did not always match those in the other groups. In particular W5 in NB did not match any consistent synergy in the other groups. The corresponding basic temporal patterns of four consistent synergies (Fig. 9*B*) were generally similar to those reported in Figs. 5, 7, and 8. Furthermore, they were often significantly wider in CA, SL, and NB relative to the controls (marked by asterisks in Fig. 9*B*). To characterize differences in timing of basic activity patterns between different groups and conditions, we computed their CoA (Fig. 9*C*, see MATERIALS AND METHODS). The CoA shifted to slightly later phases of the gait cycle in P1 for SL and NB, in P4 for NB and to earlier phase in P3 for SL. It was similar in P2 for all groups. The centers of activity of all patterns in CA were similar to those in controls. We did not compare the CoA in P5 for NB, since this pattern was not consistent across control subjects (Fig. 9, *A* and *B*).

DISCUSSION

In this study we investigated three examples of neuromuscular adjustments of gait related to postural instability. We performed the NNMF analysis on individual strides for each subject, revealing common EMG envelope features across strides. Both patients diagnosed with CA as well as healthy subjects walking on slippery surface or narrow beam exhibited a low dimensional control of spatiotemporal muscle activity. The adjustments to the neuromuscular control strategies associated with unstable gait conditions were characterized by a prolongation of basic muscle activation patterns (Figs. 5, 7, and 8) rather than by a change in the structure of muscle synergies or in the number of modules. When we compared muscle synergies and basic activation patterns between CA, SL, and NB groups, we found that they were generally consistent across subjects (Fig. 9, *A* and *B*) and similar to those reported for each task (Figs. 5, 7, and 8). Even though some differences in the FWHM or center of activity were observed across conditions, it is worth emphasizing the existence of a similar structure and widening of consistent modules in CA, SL, and NB (Figs. 5, 7, and 9). Our findings suggest that, under poor balance conditions, the prolonged activity bursts observed in many muscles result from adjustments of the same modular control strategy employed in normal walking. While the dimensionality of the modules and the structure of the weighting coefficients of synergistic muscle activation are largely preserved, the timing elements of locomotor pattern generators (including also spinal CPGs) are highly influenced by sensory/central signals.

Characteristics of CA Gait

In an attempt to compensate for large trunk oscillations and deficits in dynamic stability induced by pathology (Conte et al. 2014), patients with CA adopt some common strategies consisting in wide-base support and reduced stride length and cycle duration (Fig. 1, *A* and *B*) (Palliyath et al. 1998; Ilg et al. 2007; Serrao et al. 2012; Wuehr et al. 2013). Despite minimal differences in the mean kinematic curves between mild CA patients and healthy subjects (except for reduced ankle range of motion and increased trunk roll; Fig. 1, *A* and *B*), muscle activation patterns exhibited a remarkable increase in the duration of EMG bursts in these patients (Figs. 2*B* and 3*B*). In this regard, abnormal prolongation of EMG activity in patients with cerebellar deficits during gait was previously reported (Mari et al. 2014; Martino et al. 2014) and also observed in the upper limb muscles during elbow flexions (Hallett et al. 1975), but the modular organization of multimuscle activity coordination was not investigated before.

We found that a low dimensionality can characterize the motor patterns of CA patients, at least as far as it concerns the set of muscles studied. The number of extracted modules may indeed depend on the number of recorded muscles (Steele et al. 2013; Zelik et al. 2014). Nevertheless, for a similar set of muscles we found four modules as other authors did (Neptune et al. 2009; McGowan et al. 2010; Gizzi et al. 2011; Lacquaniti et al. 2012; De Groote et al. 2014). If one assumes four control modules, then CA patients show similar muscle weighting vectors as the controls (Fig. 5*D*), but at the same time they demonstrate altered control of patterns duration (Fig. 4*C*). In particular, three out of four basic activation patterns were characterized by a widening of the main burst (Fig. 5*E*). The smaller number of extracted basic modules found in some subjects (Fig. 5*B*) could perhaps be a result of fusion of two patterns with a close timing in the gait cycle, when they become wider. The widening of EMG bursts may explain at least in part the smaller number of modules found in some previous studies (Clark et al. 2010; Rodriguez et al. 2013), which were interpreted as resulting from merging of modules. Yet, it is worth noting that the phenomenon of widening of basic activation patterns (see Fig. 5*E*) did not depend on the exact number of modules, because it was observed even if we used three or five modules instead of four. Thus it may represent an important feature of the locomotor output in CA.

Two main alternative interpretations can be offered for the widening of the basic activity patterns in CA patients. According to the first intrepretation, the pathologic widening may highlight a fundamental contribution of cerebellum in optimizing the duration of the basic activity patterns for locomotion. Degenerative cerebellar damage might compro-

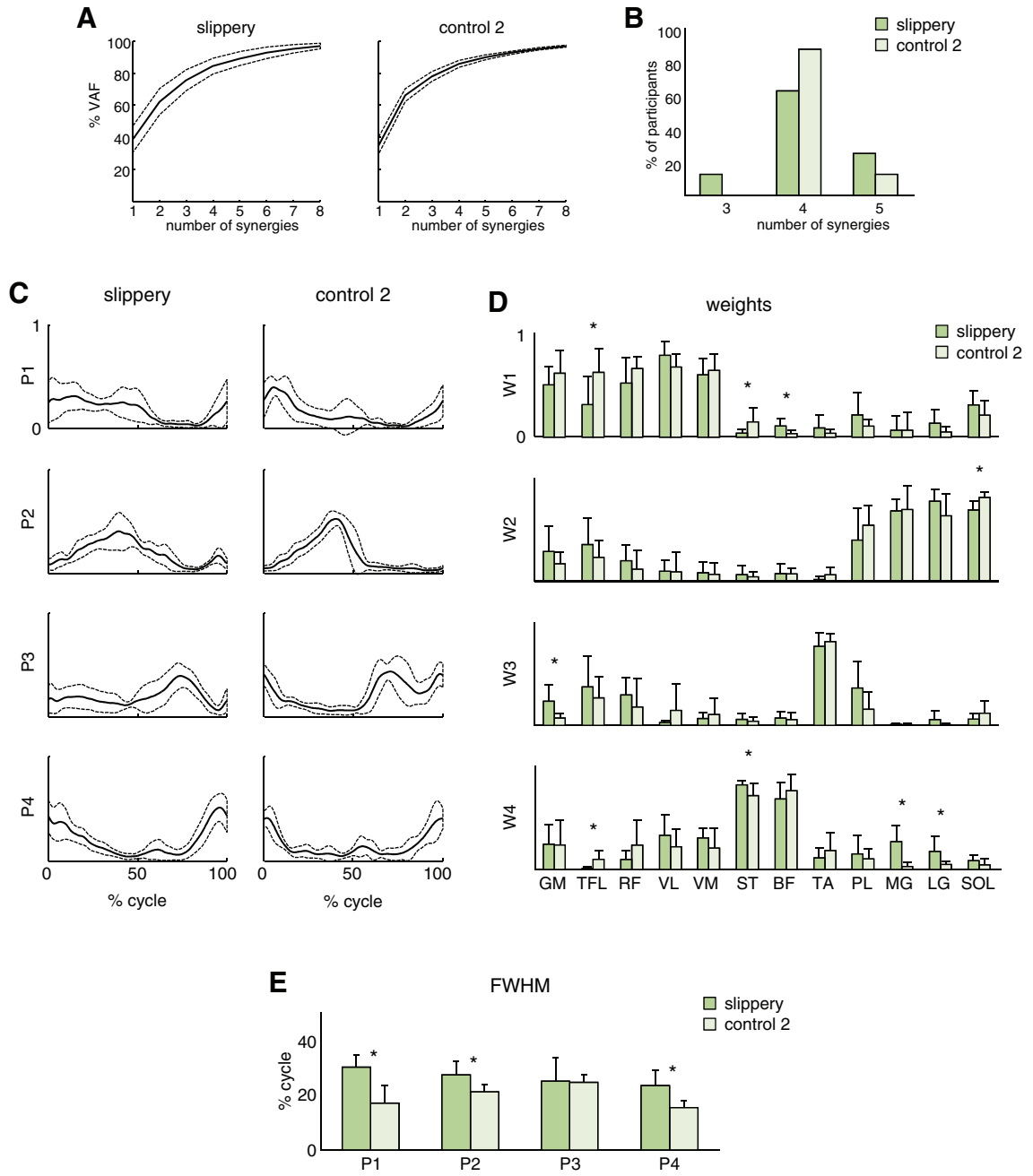

Fig. 7. Statistical analysis of EMG patterns during walking on a slippery surface using NNMF. *A*: cumulative percent of variance (VAF; ±SD) explained by basic EMG components in walking on slippery surface (*left*) and normal floor (*right*). *B*: number of modules needed to account for cycle-by-cycle variability of muscle activity estimated using the best linear fit method. *C*: ensemble-averaged basic temporal patterns (±SD) during walking on a slippery surface and normal walking with four modules assumed for each group. *D*: corresponding muscle weights. *E*: FWHM (means ± SD) of the patterns. *Significant differences. Note significant differences in components P1, P2, and P4.

mise the ability to fine tune locomotor pattern generation, as also suggested by the positive correlation between the extent of severity of pathology (clinical ataxia scale, ICARS) and the FWHM of basic patterns (Fig. 6*B*). An alternative interpretation is that the widening of the basic patterns results instead from compensatory mechanisms (Dietz 2002; Ivanenko et al. 2003; Grasso et al. 2004) adopted by the CNS to cope with the postural instability in CA. In fact, the similarity of results obtained in the manipulations of postural stability in healthy subjects (see below) seems to argue in favor of the second alternative.

Characteristics of Gait on Slippery Walkway

When subjects walked on a slippery surface, they adopted a different strategy compared with that of normal walking. Even at matched walking speeds, they used a shorter stride length and significantly reduced the range of motion of all joint angles in the sagittal plane (Fig. 1, *A* and *B*). Foot motion was characterized by slipping in the lateral direction (Cappellini et al. 2010), and systematic lateral trunk tilts took place (Fig. 1, *A* and *B*). The muscle activation patterns also differed when walking on normal and slippery surfaces (Fig. 3*C*). Neverthe-

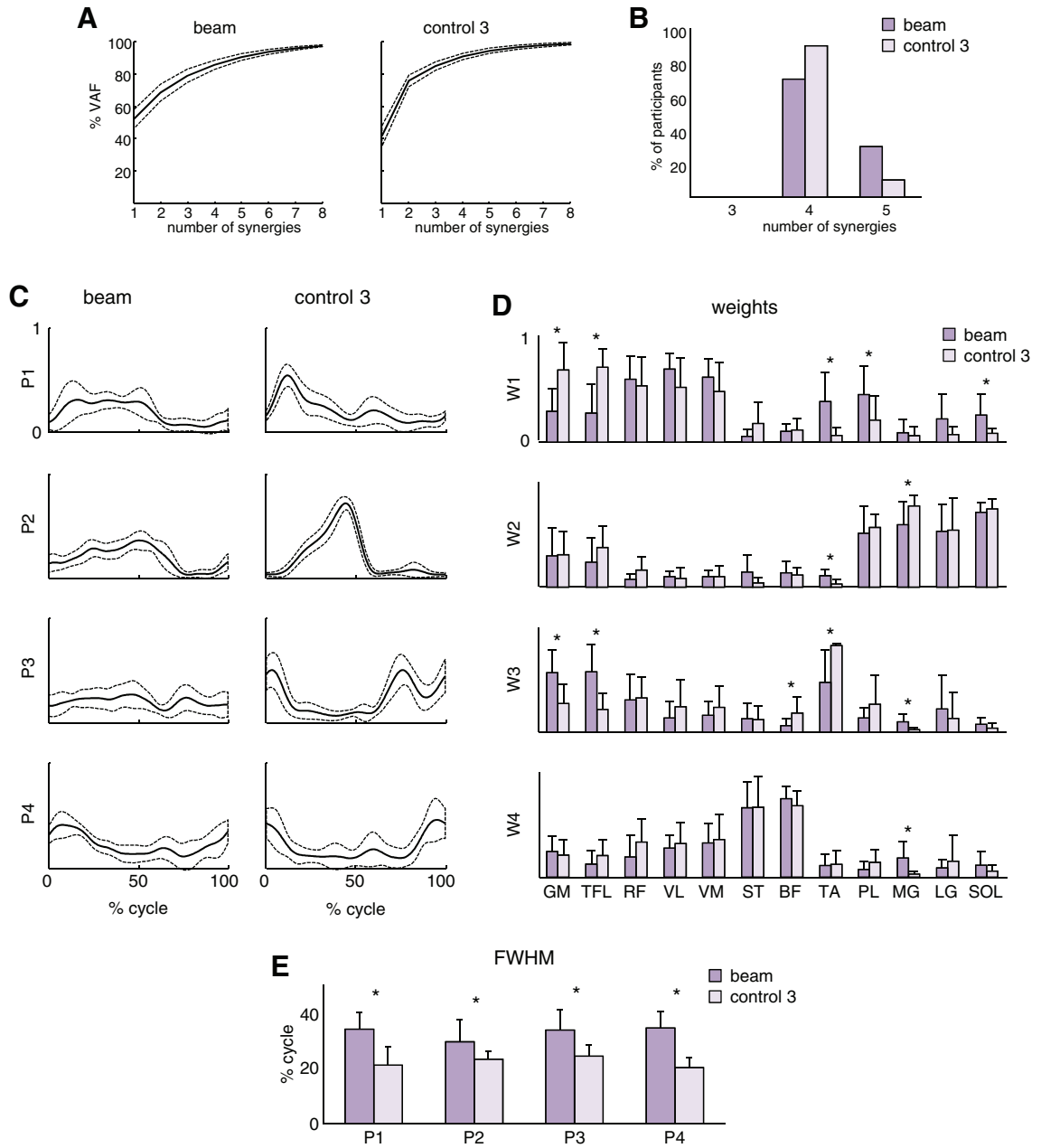

Fig. 8. Statistical analysis of EMG patterns during walking on a beam. *A*: cumulative percent of variance (VAF; ±SD) explained by basic EMG components in walking on a beam (*left*) and normal floor (*right*). *B*: number of modules needed to account for cycle-by-cycle variability of muscle activity estimated using the best linear fit method. C: ensemble-averaged basic temporal patterns (±SD) with 4 modules assumed for each group. *D*: corresponding muscle weights. *E*: FWHM (means ± SD) of the patterns. *Significant differences. Note significantly wider basic EMG components during beam walking.

less, despite some variability, the timing of activity peaks relative to the kinematic events was similar in the two conditions: activity patterns consisted of bursts of activity with a similar relationship to lift-off and touch-down events (Figs. 2 and 3*C*).

Even if the dimensionality analysis of EMGs reported some variability in the number of modules (Fig. 7*B*), on average the "best linear fit" criteria showed that EMG activity in healthy subjects on both normal or slippery surface generally was well accounted for by four modules. While Oliveira et al. (2012) demonstrated that, during gait perturbations, some adjustments in the spatial modular organization occurred (three of four modules preserved from normal walking while one module was different), here we found that the weighting vectors (muscle synergies) remained substantially unaltered (Fig. 7*D*). Nevertheless, we found that activation signals were influenced by the poor balance induced by slipping: basic patterns were characterized by a considerable widening of major bursts compared with those in normal walking. This supports the hypothesis that the CNS tunes the existing motor modules to cope with new biomechanical demands during unstable gait.

Muscle synergies and basic temporal patterns in SL were also similar to the CA group (Fig. 9) suggesting that it could be a result of task constraints and minimization of muscle effort during gait (Neptune et al. 2009; Lacquaniti et al. 2012; De Groote et al. 2014). Nonetheless, it is important to highlight

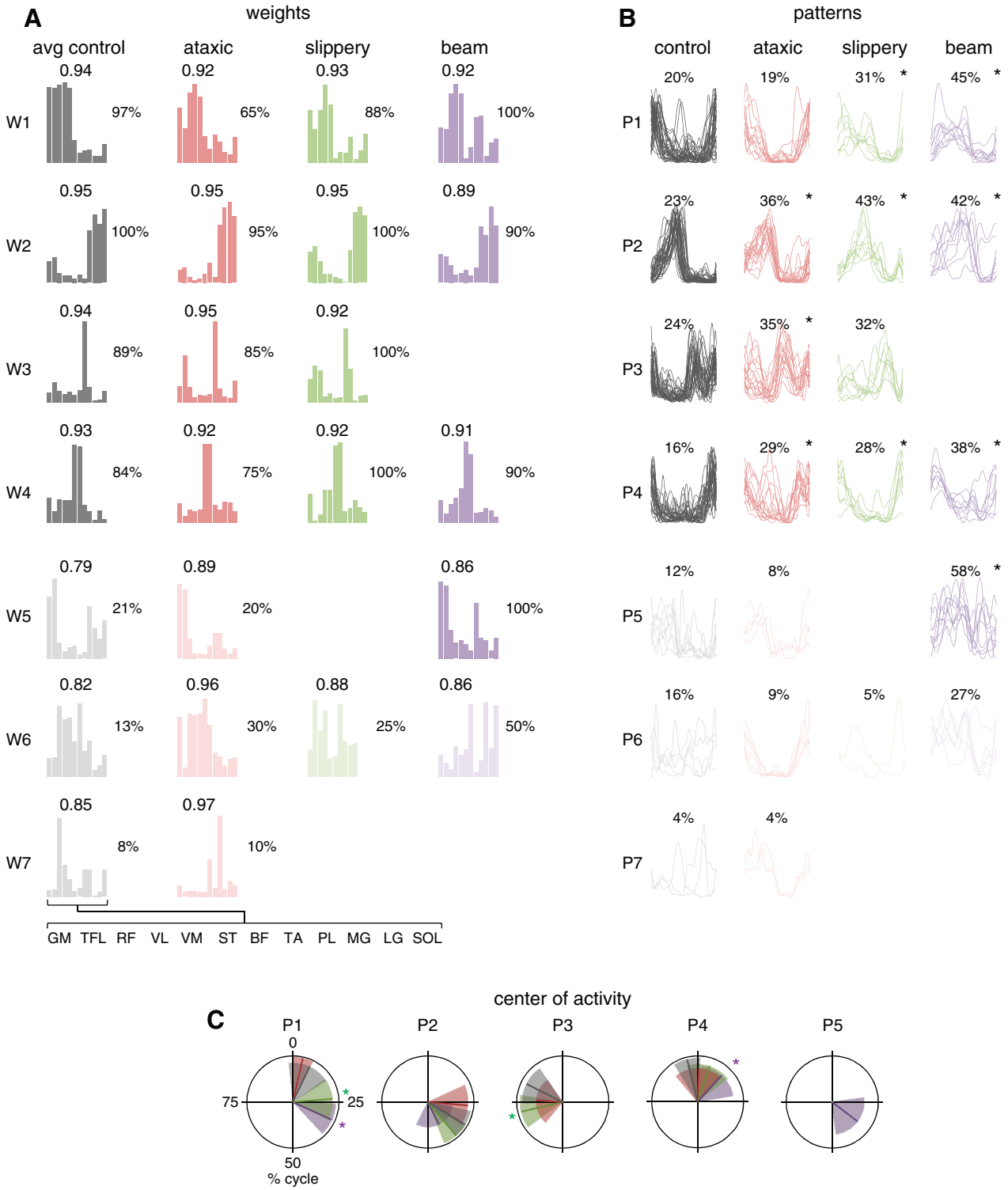

Fig. 9. Comparison of muscle module structure across different groups. *A*: group mean weights (synergies). The data for all 3 groups of control subjects were pooled together (avg control). The number of modules for each subject was not constrained to 4 but was selected based on the best linear fit method. Modules were ranked based on their best similarities (see Methods). W1, W2, W4, and W6 (and corresponding basic patterns P) were identified in each group, while W3, W5, and W7 were only identified in some groups. The numbers on the *top* of each plot represent the mean scalar product of weights of individual subjects with the group mean weight. The numbers on the *right* represent percent of subjects showing that particular synergy. Note that low values correspond to low structural consistency across subjects, and these synergies were plotted in toned-down colors. *B*: corresponding basic temporal patterns. Each curve represents the mean (across strides) pattern for an individual subject. Common (across subjects) basic patterns were plotted in a "chronological" order (with respect to the timing of the main peak), whereas inconsistent synergies were plotted separately on the *bottom*. The numbers on the top represent the mean FWHM. *C*: center of activity (CoA) of consistent basic components. The CoA vector was calculated as the 1st trigonometric moment of the circular distribution (Batschelet 1981). Polar direction denotes the relative time over the gait cycle (time progresses clockwise), and the width of the sector represents angular SD across subjects. *Significant differences compared with respective control groups.

that a prolongation of basic muscle activation patterns was a common feature of the two groups (Figs. 5, 7, and 8).

Characteristics of Beam Walking

Walking on a narrow beam represents a distinctive example of unstable gait consisting in smaller base of support (stride width), relatively smaller knee joint angle oscillations, and noticeable lateral trunk and arm movements (Fig. *1B*). The muscle activation patterns also differed significantly compared with normal walking (Figs. 2*D* and 3*D*), demonstrating a larger amount of activity in midstance.

Even though the EMG activity was more variable in NB, in most subjects its dimensionality was well captured by four modules as during normal walking (Fig. 8, *A* and *B*). The weighting vectors (muscle synergies) were generally similar between walking conditions (Fig. 8*D*), but the profiles of basic activity patterns differed (Fig. 8*C*). It is worth stressing that the FWHM was significantly greater for all basic patterns in NB than normal walking (Fig. 8*E*). It is unlikely that the lack of beam walking experience might be the primary cause for this phenomenon since, while the FWHM of P4 slightly decreased between the first and last trials in our subjects, it still remained significantly greater than that during normal walking. Also, it has been recently reported that the averaged duty cycle (activation duration) of muscle modules did not differ between experts and novices during beam walking, although experts had fewer significantly active muscles per module (Sawers and Ting 2015). Therefore, activity pattern widening may indeed represent a common feature of unstable gait (Figs. 5, 7, and 8).

Implications for Neural Control of Human Locomotion

The three examples of neuromuscular modifications suggest that, despite differences in the origin of gait instability and intrinsic putative control mechanisms, the nervous system adopts a common strategy to cope with poor balance, namely, prolonging the duration of the basic patterns of muscle activity generated by a small number of locomotor modules. The cerebellum plays an important role in balance and foot loading control (Morton and Bastian 2003; Martino et al. 2014). Moreover, sensory information related to gait is integrated by cerebellum to fine tune locomotor responses and muscle activation patterns. Both descending commands and sensory feedback influence the locomotor modules in the production of motoneuron activation patterns. Our results are also consistent with longer EMG burst durations found in cats during unstable walking (Beloozerova et al. 2010; Farrell et al. 2014) and after hindlimb deafferentation (Giuliani and Smith 1987). Thus, under unstable conditions or as a result of gait pathology the timing elements of locomotor modules, which include spinal CPGs, are highly influenced, resulting in prolonged activity bursts (Figs. 5*E*, 7*E*, and 8*E*).

The burst-like nature of the major part of the locomotor output is consistent with "drive pulse" rhythmic elements in the spinal circuitry (Kargo and Giszter 2000; Hart and Giszter 2004, 2010; Giszter et al. 2007) and with the shaping function of CPG (Patla et al. 1985; Prentice et al. 1995; Ivanenko et al. 2006). Different statistical approaches (Davis and Vaughan 1993; Olree and Vaughan 1995; Ivanenko et al. 2006; Neptune et al. 2009) converge to a similar solution about the temporal structure of the EMG activity pattern during human locomotion: the common temporal patterning elements each consist of a peak of activation at a specific timing point in the gait cycle. The burst-like activation patterns may emerge from a multilayered organization of the spinal neural networks (Prentice et al. 1995; McCrea and Rybak 2008; Lacquaniti et al. 2012): a rhythm-generation layer and a pattern-formation layer. Whatever the nature of the control/optimization of burst duration, the observed widening of basic patterns represents an interesting phenomenon that can possibly be generalized to other instable conditions.

GRANTS

This work was supported by the Italian Health Ministry, Italian Ministry of University and Research (PRIN Project), Italian Space Agency (COREA Grant), European Union FP7-ICT program (AMARSi Grant 248311), and Horizon 2020 Robotics Program (ICT-23-2014 under Grant Agreement 644727-CogIMon).

DISCLOSURES

No conflicts of interest, financial or otherwise, are declared by the author(s).

AUTHOR CONTRIBUTIONS

Author contributions: G.M., Y.P.I., A.d., M.S., A.R., F.D., C.C., and F.L. conception and design of research; G.M., Y.P.I., M.S., A.R., G.C., and C.C. performed experiments; G.M., Y.P.I., A.d., and G.C. analyzed data; G.M., Y.P.I., A.d., M.S., G.C., and F.L. interpreted results of experiments; G.M., Y.P.I., A.d., and F.L. prepared figures; G.M., Y.P.I., A.d., and F.L. drafted manuscript; G.M., Y.P.I., A.d., M.S., A.R., and F.L. edited and revised manuscript; G.M., Y.P.I., A.d., M.S., A.R., F.D., G.C., and F.L. approved final version of manuscript.

REFERENCES

Batschelet E. *Circular Statistics in Biology*. New York: Academic, 1981.

Beloozerova IN, Farrell BJ, Sirota MG, Prilutsky BI. Differences in movement mechanics, electromyographic, and motor cortex activity between accurate and nonaccurate stepping. *J Neurophysiol* 103: 2285–2300, 2010.

Berger DJ, Gentner R, Edmunds T, Pai DK, d'Avella A. Differences in adaptation rates after virtual surgeries provide direct evidence for modularity. *J Neurosci* 33: 12384–12394, 2013.

Bizzi E, Cheung VC, d'Avella A, Saltiel P, Tresch M. Combining modules for movement. *Brain Res Rev* 57: 125–133, 2008.

Bizzi E, Tresch MC, Saltiel P, d'Avella A. New perspectives on spinal motor systems. *Nat Rev Neurosci* 1: 101–108, 2000.

Borghese NA, Bianchi L, Lacquaniti F. Kinematic determinants of human locomotion. *J Physiol* 494: 863–879, 1996.

Cappellini G, Ivanenko YP, Dominici N, Poppele RE, Lacquaniti F. Motor patterns during walking on a slippery walkway. *J Neurophysiol* 103: 746–760, 2010.

Cappellini G, Ivanenko YP, Poppele RE, Lacquaniti F. Motor patterns in human walking and running. *J Neurophysiol* 95: 3426–3437, 2006.

Chamberlin ME, Fulwider BD, Sanders SL, Medeiros JM. Does fear of falling influence spatial and temporal gait parameters in elderly persons beyond changes associated with normal aging? *J Gerontol A Biol Sci Med Sci* 60: 1163–1167, 2005.

Chambers AJ, Cham R. Slip-related muscle activation patterns in the stance leg during walking. *Gait Posture* 25: 565–572, 2007.

Cheung VC, d'Avella A, Tresch MC, Bizzi E. Central and sensory contributions to the activation and organization of muscle synergies during natural motor behaviors. *J Neurosci* 25: 6419–6434, 2005.

Cheung VC, Piron L, Agostini M, Silvoni S, Turolla A, Bizzi E. Stability of muscle synergies for voluntary actions after cortical stroke in humans. *Proc Natl Acad Sci USA* 106: 19563–19568, 2009.

Chvatal SA, Ting LH. Voluntary and reactive recruitment of locomotor muscle synergies during perturbed walking. *J Neurosci* 32: 12237–12250, 2012.

Clark DJ, Ting LH, Zajac FE, Neptune RR, Kautz SA. Merging of healthy motor modules predicts reduced locomotor performance and muscle coordination complexity post-stroke. *J Neurophysiol* 103: 844–857, 2010.

Conte C, Pierelli F, Casali C, Ranavolo A, Draicchio F, Martino G, Harfoush M, Padua L, Coppola G, Sandrini G, Serrao M. Upper body kinematics in patients with cerebellar ataxia. *Cerebellum* 13: 689–697, 2014.

Courtine G, Papaxanthis C, Schieppati M. Coordinated modulation of locomotor muscle synergies constructs straight-ahead and curvilinear walking in humans. *Exp Brain Res* 170: 320–335, 2006.

d'Avella A, Portone A, Fernandez L, Lacquaniti F. Control of fast-reaching movements by muscle synergy combinations. *J Neurosci* 26: 7791–7810, 2006.

d'Avella A, Saltiel P, Bizzi E. Combinations of muscle synergies in the construction of a natural motor behavior. *Nat Neurosci* 6: 300–308, 2003.

Danner SM, Hofstoetter US, Freundl B, Binder H, Mayr W, Rattay F, Minassian K. Human spinal locomotor control is based on flexibly organized burst generators. *Brain* 138: 577–588, 2015.

Davis BL, Vaughan CL. Phasic behavior of EMG signals during gait: use of multivariate statistics. *J Electromyogr Kinesiol* 3: 51–60, 1993.

De Groote F, Jonkers I, Duysens J. Task constraints and minimization of muscle effort result in a small number of muscle synergies during gait. *Front Comput Neurosci* 8: 115, 2014.

Dietz V. Proprioception and locomotor disorders. *Nat Rev Neurosci* 3: 781–790, 2002.

Dingwell JB, Cusumano JP, Sternad D, Cavanagh PR. Slower speeds in patients with diabetic neuropathy lead to improved local dynamic stability of continuous overground walking. *J Biomech* 33: 1269–1277, 2000.

Dominici N, Ivanenko YP, Cappellini G, d'Avella A, Mondì V, Cicchese M, Fabiano A, Silei T, Di Paolo A, Giannini C, Poppele RE, Lacquaniti F. Locomotor primitives in newborn babies and their development. *Science* 334: 997–999, 2011.

Drew T, Kalaska J, Krouchev N. Muscle synergies during locomotion in the cat: a model for motor cortex control. *J Physiol* 586: 1239–1245, 2008.

Earhart GM, Bastian AJ. Selection and coordination of human locomotor forms following cerebellar damage. *J Neurophysiol* 85: 759–769, 2001.

Farrell BJ, Bulgakova MA, Beloozerova IN, Sirota MG, Prilutsky BI. Body stability and muscle and motor cortex activity during walking with wide stance. *J Neurophysiol* 112: 504–524, 2014.

Flanders M. What is the biological basis of sensorimotor integration? *Biol Cybern* 104: 1–8, 2011.

Fox EJ, Tester NJ, Kautz SA, Howland DR, Clark DJ, Garvan C, Behrman AL. Modular control of varied locomotor tasks in children with incomplete spinal cord injuries. *J Neurophysiol* 110: 1415–1425, 2013.

Giszter SF, Hart CB, Silfies SP. Spinal cord modularity: evolution, development, and optimization and the possible relevance to low back pain in man. *Exp Brain Res* 200: 283–306, 2010.

Giszter S, Patil V, Hart C. Primitives, premotor drives, and pattern generation: a combined computational and neuroethological perspective. *Prog Brain Res* 165: 323–346, 2007.

Giuliani CA, Smith JL. Stepping behaviors in chronic spinal cats with one hindlimb deafferented. *J Neurosci* 7: 2537–2546, 1987.

Gizzi L, Nielsen JF, Felici F, Ivanenko YP, Farina D. Impulses of activation but not motor modules are preserved in the locomotion of subacute stroke patients. *J Neurophysiol* 106: 202–210, 2011.

Grasso R, Ivanenko YP, Zago M, Molinari M, Scivoletto G, Castellano V, Macellari V, Lacquaniti F. Distributed plasticity of locomotor pattern generators in spinal cord injured patients. *Brain* 127: 1019–1034, 2004.

Grillner S. Neuroscience. Human locomotor circuits conform. *Science* 334: 912–913, 2011.

Grönqvist R, Hirvonen M, Tuusa A. Slipperiness of the shoe-floor interface: comparison of objective and subjective assessments. *Appl Ergon* 24: 258–262, 1993.

Hallett M, Shahani BT, Young RR. EMG analysis of patients with cerebellar deficits. *J Neurol Neurosurg Psychiatry* 38: 1163–1169, 1975.

Hart CB, Giszter SF. Modular premotor drives and unit bursts as primitives for frog motor behaviors. *J Neurosci* 24: 5269–5282, 2004.

Hart CB, Giszter SF. A neural basis for motor primitives in the spinal cord. *J Neurosci* 30: 1322–1336, 2010.

Hayes HB, Chvatal SA, French MA, Ting LH, Trumbower RD. Neuromuscular constraints on muscle coordination during overground walking in persons with chronic incomplete spinal cord injury. *Clin Neurophysiol* 125: 2024–2035, 2014.

Heiden TL, Sanderson DJ, Inglis JT, Siegmund GP. Adaptations to normal human gait on potentially slippery surfaces: the effects of awareness and prior slip experience. *Gait Posture* 24: 237–246, 2006.

Ilg W, Giese MA, Gizewski ER, Schoch B, Timmann D. The influence of focal cerebellar lesions on the control and adaptation of gait. *Brain* 131: 2913–2927, 2008.

Ilg W, Golla H, Thier P, Giese MA. Specific influences of cerebellar dysfunctions on gait. *Brain* 130: 786–798, 2007.

Ivanenko YP, Cappellini G, Dominici N, Poppele RE, Lacquaniti F. Coordination of locomotion with voluntary movements in humans. *J Neurosci* 25: 7238–7253, 2005.

Ivanenko YP, Cappellini G, Solopova IA, Grishin AA, MacLellan MJ, Poppele RE, Lacquaniti F. Plasticity and modular control of locomotor patterns in neurological disorders with motor deficits. *Front Comput Neurosci* 7: 123, 2013.

Ivanenko YP, Dominici N, Lacquaniti F. Development of independent walking in toddlers. *Exerc Sport Sci Rev* 35: 67–73, 2007.

Ivanenko YP, Grasso R, Zago M, Molinari M, Scivoletto G, Castellano V, Macellari V, Lacquaniti F. Temporal components of the motor patterns expressed by the human spinal cord reflect foot kinematics. *J Neurophysiol* 90: 3555–3565, 2003.

Ivanenko YP, Poppele RE, Lacquaniti F. Five basic muscle activation patterns account for muscle activity during human locomotion. *J Physiol* 556: 267–282, 2004.

Ivanenko YP, Poppele RE, Lacquaniti F. Motor control programs and walking. *Neuroscientist* 12: 339–348, 2006.

Kargo WJ, Giszter SF. Rapid correction of aimed movements by summation of force-field primitives. *J Neurosci* 20: 409–426, 2000.

Kautz SA, Bowden MG, Clark DJ, Neptune RR. Comparison of motor control deficits during treadmill and overground walking poststroke. *Neurorehabil Neural Repair* 25: 756–765, 2011.

Lacquaniti F, Ivanenko YP, Zago M. Patterned control of human locomotion. *J Physiol* 590: 2189–2199, 2012.

Lee DD, Seung HS. Algorithms for non-negative matrix factorization. In: *Advances in Neural Information Processing Systems*, edited by Leen TK, Dietterich TG, Tresp V. Cambridge, MA: MIT Press, 2001, vol. 13, p. 556–562.

Levine AJ, Hinckley CA, Hilde KL, Driscoll SP, Poon TH, Montgomery JM, Pfaff SL. Identification of a cellular node for motor control pathways. *Nat Neurosci* 17: 586–593, 2014.

Maki BE. Gait changes in older adults: predictors of falls or indicators of fear. *J Am Geriatr Soc* 45: 313–320, 1997.

Mari S, Serrao M, Casali C, Conte C, Martino G, Ranavolo A, Coppola G, Draicchio F, Padua L, Sandrini G, Pierelli F. Lower limb antagonist muscle co-activation and its relationship with gait parameters in cerebellar ataxia. *Cerebellum* 13: 226–236, 2014.

Martino G, Ivanenko YP, Serrao M, Ranavolo A, d'Avella A, Draicchio F, Conte C, Casali C, Lacquaniti F. Locomotor patterns in cerebellar ataxia. *J Neurophysiol* 112: 2810–2821, 2014.

McAndrew Young PM, Dingwell JB. Voluntary changes in step width and step length during human walking affect dynamic margins of stability. *Gait Posture* 36: 219–224, 2012.

McCrea DA, Rybak IA. Organization of mammalian locomotor rhythm and pattern generation. *Brain Res Rev* 57: 134–146, 2008.

McGowan CP, Neptune RR, Clark DJ, Kautz SA. Modular control of human walking: Adaptations to altered mechanical demands. *J Biomech* 43: 412–419, 2010.

Mitoma H, Hayashi R, Yanagisawa N, Tsukagoshi H. Characteristics of parkinsonian and ataxic gaits: a study using surface electromyograms, angular displacements and floor reaction forces. *J Neurol Sci* 174: 22–39, 2000.

Monaco V, Ghionzoli A, Micera S. Age-related modifications of muscle synergies and spinal cord activity during locomotion. *J Neurophysiol* 104: 2092–2102, 2010.

Monaco V, Martelli D, Nacci A, Fattori B, Berrettini S, Micera S. Modifications of muscle synergies and spinal maps due to absence of visual feedback in patients with unilateral vestibular disease. *Conf Proc IEEE Eng Med Biol Soc* 2012: 3608–3611, 2012.

Morton SM, Bastian AJ. Relative contributions of balance and voluntary leg-coordination deficits to cerebellar gait ataxia. *J Neurophysiol* 89: 1844–1856, 2003.

Morton SM, Bastian AJ. Cerebellar control of balance and locomotion. *Neuroscientist* 10: 247–259, 2004.

Neptune RR, Clark DJ, Kautz SA. Modular control of human walking: a simulation study. *J Biomech* 42: 1282–1287, 2009.

Oliveira ASC, Gizzi L, Kersting UG, Farina D. Modular organization of balance control following perturbations during walking. *J Neurophysiol* 108: 1895–1906, 2012.

Oliveira AS, Gizzi L, Farina D, Kersting UG. Motor modules of human locomotion: influence of EMG averaging, concatenation, and number of step cycles. *Front Hum Neurosci* 8: 335, 2014.

Olree KS, Vaughan CL. Fundamental patterns of bilateral muscle activity in human locomotion. *Biol Cybern* 73: 409–414, 1995.

Palliyath S, Hallett M, Thomas SL, Lebiedowska MK. Gait in patients with cerebellar ataxia. *Mov Disord* 13: 958–964, 1998.

Patla AE, Calvert TW, Stein RB. Model of a pattern generator for locomotion in mammals. *Am J Physiol Regul Integr Comp Physiol* 248: R484–R494, 1985.

Prentice SD, Patla AE, Stacey DA. Modelling the time-keeping function of the central pattern generator for locomotion using artificial sequential neural network. *Med Biol Eng Comput* 33: 317–322, 1995.

Redfern MS, Cham R, Gielo-Perczak K, Grönqvist R, Hirvonen M, Lanshammar H, Marpet M, Pai CY, Powers C. Biomechanics of slips. *Ergonomics* 44: 1138–1166, 2001.

Rodriguez KL, Roemmich RT, Cam B, Fregly BJ, Hass CJ. Persons with Parkinson's disease exhibit decreased neuromuscular complexity during gait. *Clin Neurophysiol* 124: 1390–1397, 2013.

Routson RL, Kautz SA, Neptune RR. Modular organization across changing task demands in healthy and poststroke gait. *Physiol Rep* 2: e12055, 2014.

Safavynia SA, Ting LH. Task-level feedback can explain temporal recruitment of spatially fixed muscle synergies throughout postural perturbations. *J Neurophysiol* 107: 159–177, 2012.

Sawers A, Ting L. *Expertise alters the modular organization of walking balance control. Society for the Neural Control of Movement 25th Annual Meeting*. Charleston, SC: Soc. Neural Control Movement, 2015.

Serrao M, Pierelli F, Ranavolo A, Draicchio F, Conte C, Don R, Di Fabio R, LeRose M, Padua L, Sandrini G, Casali C. Gait pattern in inherited cerebellar ataxias. *Cerebellum* 11: 194–211, 2012.

Steele KM, Tresch MC, Perreault EJ. The number and choice of muscles impact the results of muscle synergy analyses. *Front Comput Neurosci* 7: 105, 2013.

Stolze H, Klebe S, Petersen G, Raethjen J, Wenzelburger R, Witt K, Deuschl G. Typical features of cerebellar ataxic gait. *J Neurol Neurosurg Psychiatry* 73: 310–312, 2002.

Strandberg L. On accident analysis and slip-resistance measurement. *Ergonomics* 26: 11–32, 1983.

Sylos-Labini F, La Scaleia V, d'Avella A, Pisotta I, Tamburella F, Scivoletto G, Molinari M, Wang S, Wang L, van Asseldonk E, van der Kooij H, Hoellinger T, Cheron G, Thorsteinsson F, Ilzkovitz M, Gancet J, Hauffe R, Zanov F, Lacquaniti F, Ivanenko YP. EMG patterns during assisted walking in the exoskeleton. *Front Hum Neurosci* 8: 423, 2014.

Torres-Oviedo G, Macpherson JM, Ting LH. Muscle synergy organization is robust across a variety of postural perturbations. *J Neurophysiol* 96: 1530–1546, 2006.

Torres-Oviedo G, Ting LH. Subject-specific muscle synergies in human balance control are consistent across different biomechanical contexts. *J Neurophysiol* 103: 3084–3098, 2010.

Tresch MC, Saltiel P, d'Avella A, Bizzi E. Coordination and localization in spinal motor systems. *Brain Res Brain Res Rev* 40: 66–79, 2002.

Trouillas P, Takayanagi T, Hallett M, Currier RD, Subramony SH, Wessel K, Bryer A, Diener HC, Massaquoi S, Gomez CM, Coutinho P, Ben Hamida M, Campanella G, Filla A, Schut L, Timann D, Honnorat J, Nighoghossian N, Manyam B. International Cooperative Ataxia Rating Scale for pharmacological assessment of the cerebellar syndrome. The Ataxia Neuropharmacology Committee of the World Federation of Neurology. *J Neurol Sci* 145: 205–211, 1997.

Vasudevan EV, Torres-Oviedo G, Morton SM, Yang JF, Bastian AJ. Younger is not always better: development of locomotor adaptation from childhood to adulthood. *J Neurosci* 31: 3055–3065, 2011.

Watson GS, Williams EJ. On the construction of significance tests on the circle and the sphere. *Biometrika* 43: 344–352, 1956.

Wuehr M, Schniepp R, Ilmberger J, Brandt T, Jahn K. Speed-dependent temporospatial gait variability and long-range correlations in cerebellar ataxia. *Gait Posture* 37: 214–218, 2013.

Zelik KE, La Scaleia V, Ivanenko YP, Lacquaniti F. Can modular strategies simplify neural control of multidirectional human locomotion? *J Neurophysiol* 111: 1686–1702, 2014.